Title

Detection of Frog virus 3 by integrating RPA-CRISPR/Cas12a-SPM with deep learning

Authors

Zhengyang Lei [a, b, †], Lijin Lian [a, b, †], Likun Zhang [a, b, †], Changyue Liu [a, b], Shiyao Zhai [a, b], Xi Yuan [a, b], Jiazhang Wei [c], Hong Liu [d], Ying Liu [d], Zhicheng Du [a, b], Ijaz Gul [a, b], Haihui Zhang [a, b], Zhifeng Qin [e], Shaoling Zeng [e], Peng Jia [f], Ke Du [g], Lin Deng [h], Dongmei Yu [i, *], Qian He [a, b], Peiwu Qin [a, b, *]

*Email: pwqin@sz.tsinghua.edu.cn. Address: Lishui Road 2199, Nanshan District, Shenzhen, China 518055.
†This author contributed equally to this paper

Affiliations

[a] *Center of Precision Medicine and Healthcare, Tsinghua-Berkeley Shenzhen Institute, Shenzhen, Guangdong Province, 518055, China.*

[b] *Institute of Biopharmaceutics and Health Engineering, Tsinghua Shenzhen International Graduate School, Shenzhen, Guangdong Province, 518055, China.*

[c] *Department of Otolaryngology & Head and Neck, The People's Hospital of Guangxi Zhuang Autonomous Region, Guangxi Academy of Medical Sciences, 6 Taoyuan Road, Nanning, 530021, China.*

[d] *Animal and Plant Inspection and Quarantine Technical Centre, Shenzhen Exit and Entry Inspection and Quarantine Bureau, Guangdong Province, 518045, China.*

[e] *Animal and Plant Inspection and Quarantine Technology Center, Shenzhen Customs, Shenzhen, Guangdong Province, 518033, China.*

[f] *Quality and Standards Academy, Shenzhen Technology University, Shenzhen 518118, China.*

[g] *Department of Chemical and Environmental Engineering, University of California, Riverside, 92521, United States.*

[h] *Shenzhen Bay Laboratory, Shenzhen, 518132, China.*

[i] *School of Mechanical, Electrical & Information Engineering, Shandong University, Weihai, Shandong, 264209, China.*

Table S1 Oligonucleotides used in this study.

FV3 MCP	5'-ATGTCTTCTGTAACTGGTTCAGGTATCACAAGTGGTTTCATCGACTTGGCCACTTATGACAATCTTGAGAGAGCAATGTACGGGGGGTTCGGACGCCACCACGTACTTTGTCAAGGAGCACTACCCCGTGGGGTGGTTCACCAAGCTGCCGTCTCTGGCTGCCAAGATGTCGGGTAACCCGGCTTTCGGGCAGCAGTTTTCGGTCGGCGTTCCCAGGTCGGGGGGATTACATCCTCAACGCC -3' (240bp)
ISKNV MCP	5'-ATGTCTGCAATCTCAGGTGCAAACGTAACCAGCGGGTTCATCGACATCTCCGCGTTTGATGCGATGGAGACCCACTTGTACGGCGGCGACAATGCCGTGACCTACTTTGCCCGTGAGACCGTGCGTAGTTCCTGGTACAGCAAACTGCCCGTCACCCTGTCAAAACAGACTGGCCATGCCAATTTTGGGCAGGAGTTTAGTGTGACGGTGGCGAGGGGCGGCGACTACCTC -3' (231bp)
RPA primer F1	ATGTCTTCTGTAACTGGTTCAGGTATCACAAG
RPA primer F2	ATGTCTTCTGTAACTGGTTCAGGTATCACA
RPA primer F3	TCTTCTGTAACTGGTTCAGGTATCACAAGTGGT
RPA primer R1	GGCGTTGAGGATGTAATCCCCCGACCTGGG
RPA primer R2	GGCGTTGAGGATGTAATCCCCCGACCTGGGAA
RPA primer R3	CGTTGAGGATGTAATCCCCCGACCTGGGAACG
FV3 MCP PCR-F	ATGTCTTCTGTAACTGGTTCA
FV3 MCP PCR-R	GGCGTTGAGGATGTAATCCCC
ISKNV MCP F	ATGTCTGCAATCTCAGGTGC
ISKNV MCP R	GAGGTAGTCGCCGCCCCT
MCP qPCR-F	GGTTCAGGTATCACAAGTGGT
MCP qPCR-R	GCGTTGAGGATGTAATCCC
LbCas12a crRNA-1	uaauuucuacuaaguguagauATCGACTTGGCCACTTATGACAA
LbCas12a crRNA-2	uaauuucuacuaaguguagauTCAAGGAGCACTACCCCGTGGGG
LbCas12a crRNA-3	uaauuucuacuaaguguagauGGGCAGCAGTTTTCGGTCGGCGT
ssDNA reporter	/5TAMRA/TTATT/3BHQ2

Table S2 The information of animal-derived samples used in this study.

Pathogens	Host	Region	Refs
Tiger frog virus	Rana tigrina rugulosa	Guangdong, China	Unpublished
Soft-shelled turtle iridovirus	Trionyx Sinensis	Guangdong, China	Zhao et al. 2007
Bohle iridovirus	Emydura krefftii	Guangdong, China	Unpublished
Rana Grylio iridovirus	Rana Grylio	Guangdong, China	Unpublished

Table S3 Deep learning models performance for binary classification.

Models / Index	DenseNet-121	AlexNet	EfficientNet-B7
Accuracy	100.00%	100.00%	100.00%
Precision	100.00%	100.00%	100.00%
Recall	100.00%	100.00%	100.00%
F1 Score	100.00%	100.00%	100.00%
Inference Time	38ms	24ms	48ms

Table S4 Deep learning models performance for multiclass classification.

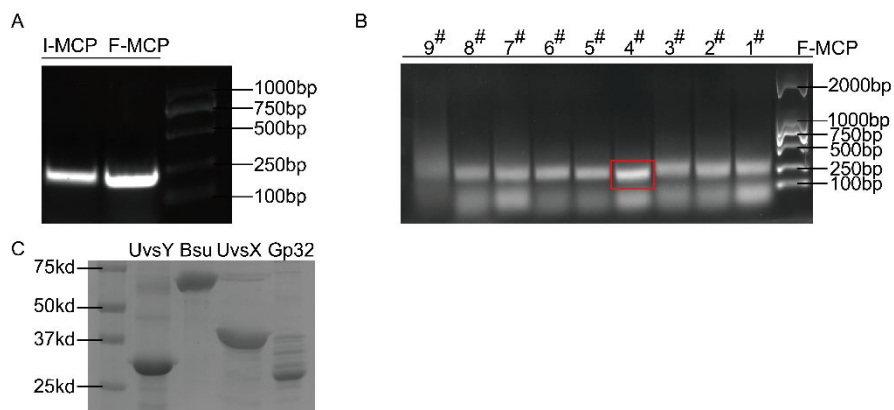| Models / Index	DenseNet-121	AlexNet	EfficientNet-B7
Accuracy	97.50%	98.75%	97.50%
Precision	97.67%	98.85%	97.66%
Recall	97.50%	98.75%	97.50%
F1 Score	97.48%	98.75%	97.47%
Inference Time	31ms	15ms	41ms

Figure S1. Optimization of RPA primers and crRNA. **(A)** Agarose gel electrophoresis for purified target and control fragment. I-MCP: ISKNV MCP, F-MCP: FV3 MCP. **(B)** Result of agarose gel electrophoresis for evaluation of RPA efficiency. 1 nM purified target is used. 1[#] represents RPA primer F1 and RPA primer R1. The 4th pair of primers shows better amplification efficiency (RPA primer F2 and RPA primer R1). **(C)** The molecular weight of purified proteins for RPA is confirmed by SDS-PAGE.
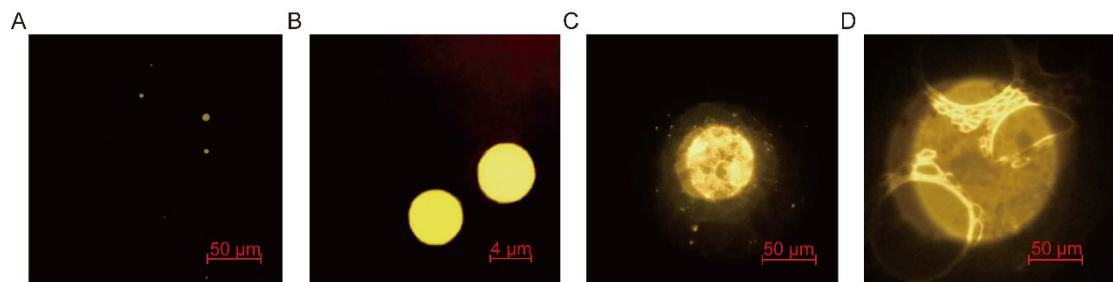

Figure S2. Images of standard samples with SPM. **(A)** Detection of mixture beads with the diameter of 0.1 μm, 0.2 μm, 0.5 μm, 1 μm, and 4 μm (TstraSpeck Fluorescent Microspheres Size Kit (T14792)). The excitation

wavelength and the emission wavelength are 560 nm and 580 nm, respectively. **(B)** The image of 4 μm fluorescent beads. **(C)** The image of the potato's underground stem. **(D)** The image of the potato's stem tube
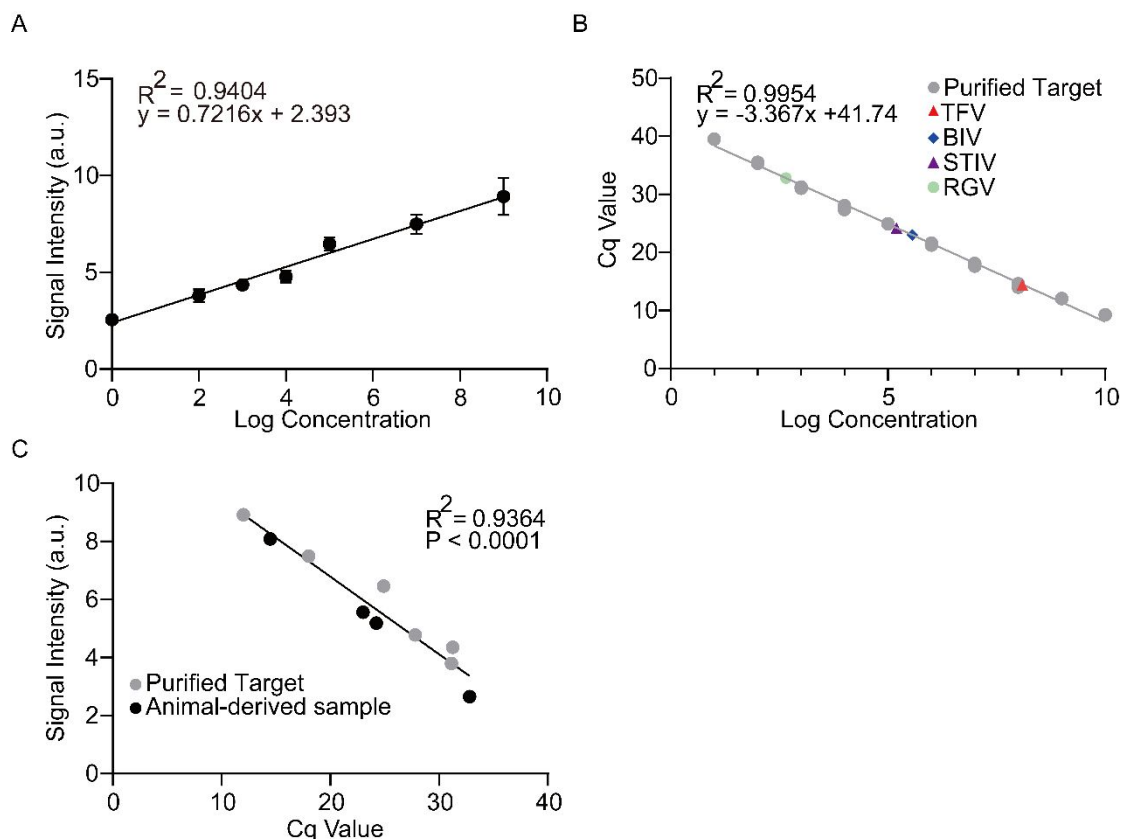
A

B

C

Figure S3. Standard curve of the proposed system and qPCR. **(A)** Concentration-signal intensity curve of DNA concentration and smartphone images. The standard samples with purified target DNA of 10 aM, 100 aM, 1fM, 10 fM, 1 pM, 100 pM, and control DNA of 100 pM are detected by crRNA-3 with RPA-CRISPR/Cas12a-smartphone microscopy**. (B)** Concentration-signal intensity curve of qPCR. The standard samples with purified target DNA of 1 aM, 10 aM, 100 aM, 1 fM, 10 fM, 10 pM, 100 pM, 1 nM, are detected by qPCR. The concentration of each clinical sample is estimated according to this calibration curve. (C) The correlation analysis of FV3 detection results obtained through RPA-CRISPR/Cas12a-SPM system and qPCR. The fluorescence signal intensity and Cq value of each sample are co-analyzed.
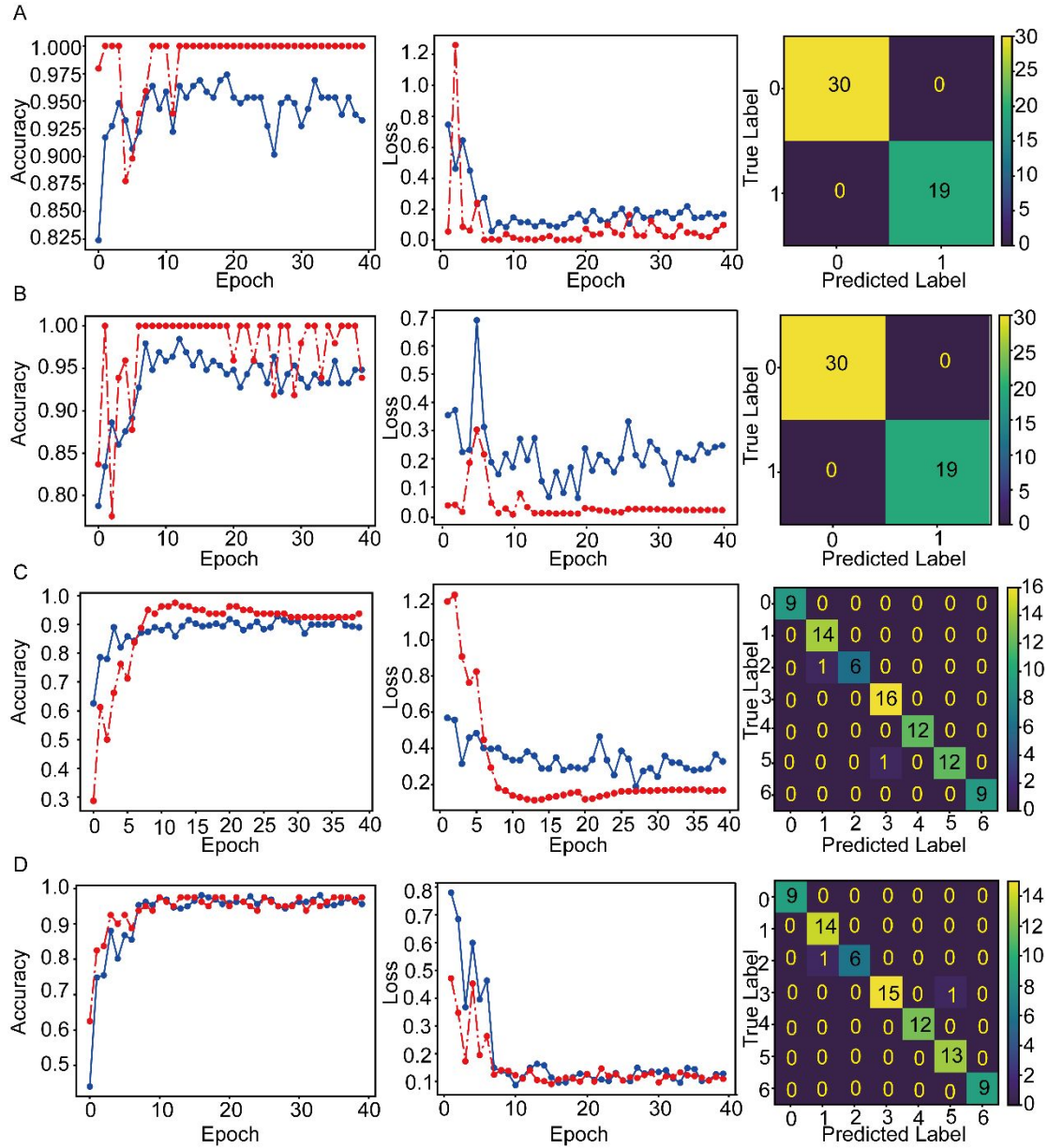
Figure S4. Evaluation of Deep learning models for classification of fluorescence images. **(A)** Evaluation of DenseNet-121 for binary classification. **(B)** Evaluation of AlexNet for binary classification. **(C)** Evaluation of efficienctNet-B7 for multiclass classification. **(D)** Evaluation of DenseNet-121 for multiclass classification.